

# $\Lambda$ hyperonic effect on the magnesium dripline

Torsten Schürhoff

*Frankfurt Institute for Advanced Studies(FIAS), Institute for Theoretical Physics(ITP),  
Johann Wolfgang Goethe University, Frankfurt am Main, Germany*

Stefan Schramm

*Frankfurt Institute for Advanced Studies(FIAS), Institute for Theoretical Physics(ITP),  
Center for Scientific Computing(CSC), Johann Wolfgang Goethe University, Frankfurt am Main, Germany*

Chhanda Samanta

*Department of Physics and Astronomy, Virginia Military Institute, Lexington, VA 24450, USA*

(Dated: November 27, 2024)

Neutron dripline calculations for both magnesium nuclei and magnesium +  $\Lambda$  hypernuclei have been carried out in a microscopic framework using a chiral effective model. The results are compared with two other relativistic mean field models, SPL-40 and NL3. All three models describe the  $\Lambda$  separation energy of known hypernuclei adequately. The extrapolation to the driplines for moderately heavy hypernuclei are found to be strongly model-dependent.

PACS numbers:

## I. INTRODUCTION

Hypernuclei are of particular interest in nuclear physics and nuclear astrophysics. Hyperons, consisting of up, down and strange quarks, have a very short life time on the weak-interaction timescale ( $\sim 10^{-10}s$ ) and can form a bound system with nucleons. Thus they can supply the most direct information on the interaction of hyperons in nuclear matter, which is also essential for the study and possible masses of neutron stars.

The hyperon is not Pauli-blocked by the nucleons and thus can occupy the lowest energy level while providing extra binding. This can make an unbound normal nucleus bound (viz., the nucleus  ${}^9Li + n$  is unbound, but  ${}^9Li + \Lambda$  is bound), and may even lead to the production of exotic nuclei beyond the normal drip lines. Hence hypernuclei are an experimental testing ground to study how a system of up- and down-quarks changes towards the full flavor SU(3), when strange quarks are added implicitly through hyperons.

The binding energy of various hypernuclei has already been measured. To increase this number, experimental searches for neutron rich hypernuclei have been carried out at JPARC, Japan [1], [2], and JLab, USA [3], [4]. Also, there are proposed experiments like HypHI [5], [6] at GSI, Darmstadt, Germany and NICA [7] in Dubna, Russia. A review of some of the future research activities can be found in [8]. These proposed experiments will probe higher-mass hypernuclei and investigate neutron-rich hyper nuclei towards the hypernuclear neutron dripline, similar to investigations into the nuclear dripline.

In this context we present a study of the position of the drip line of magnesium isotopes and consider the impact of an additional  $\Lambda$  hyperon on neutron-rich isotopes. The calculations are based on a new parameterization of a well-established SU(3) chiral effective approach for

studying hadronic matter and nuclei. The results are compared to two different relativistic Walecka-type models, SPL-40 [9],[10] and NL3 [11].

The outline of the paper is as following: in section 2 the chiral model used for our calculation is described. In section 3 we show the results for the dripline calculations. In section 4 the results are discussed and we give a conclusion.

## II. DESCRIPTION OF THE MODEL

The Frankfurt chiral model uses an effective SU(3) sigma-omega model approach to describe nuclear physics. A first version of the model was developed in [12] [13] and has been stepwise expanded to describe cross-checks with heavy-ion experiments [14], the inclusion of higher baryon resonances [15] and neutron star physics [16].

In a paper preceding this work [17], nuclear binding energies were fitted. While this approach gives good results for nuclear binding energies, it also produces a maximum neutron star mass of just  $1.64 M_{\odot}$ . More recent neutron star mass measurements by Demorest et al. [18] and Antoniadis et al. [19] point to a maximum mass of neutron stars of at least  $1.97 \pm 0.04 M_{\odot}$  or  $2.01 \pm 0.04 M_{\odot}$ .

In order to keep the model up-to-date, certain key parameters have been reexamined. Among them are the nucleon-omega meson coupling ( $g_{N\omega}$ ), the nucleon-rho meson coupling  $g_{N\rho}$ , the vector-meson self-interaction  $g_4^4$  and several other model parameters.

The degrees of freedom included in the model are the baryon octet (n,p, and hyperons  $\Lambda, \Sigma^{+,0,-}, \Xi^{0,-}$ ) and the leptons (e,  $\mu$ ). The model uses an effective approach where the mesons mediate the interactions between the baryons. The relevant mesonic degrees of freedom in the mean-field calculation performed in these studies are the vector-isoscalar  $\omega$  and  $\phi$ , the vector-isovector  $\rho$  and the

scalar-isoscalar  $\sigma$  and  $\zeta$  (strange quark-antiquark state).

The Lagrangian density contains the following terms

$$L = L_{Kin} + L_{Int} + L_{Self} + L_{SB}, \quad (1)$$

where  $L_{Kin}$  is the kinetic energy term for the hadrons. In addition there is an interaction term between the baryons and the scalar and vector mesons

$$L_{Int} = - \sum_i \bar{\psi}_i [\gamma_0 (g_{i\omega}\omega + g_{i\phi}\phi + g_{i\rho}\tau_3\rho) + M_i^*] \psi_i, \quad (2)$$

with the effective mass  $M_i^*$  given by

$$M_i^* = g_{i\sigma}\sigma + g_{i\zeta}\zeta + \delta m_i. \quad (3)$$

with a small bare mass term  $\delta m_i$ . The coupling strengths of the baryons to the scalar fields are connected via SU(3) symmetry relations and the different SU(3) invariant coupling strengths are fitted to reproduce the baryon masses in vacuum (see ref. [16] for the values of the couplings). The self-interaction terms for the scalar mesons read

$$\begin{aligned} \mathcal{L}_{Scalar} = & \frac{1}{2}k_0\chi^2(\sigma^2 + \zeta^2 + \delta^2) - k_1(\sigma^2 + \zeta^2 + \delta^2)^2 \\ & - k_2\left(\frac{\sigma^4}{2} + \frac{\delta^4}{2} + 3\sigma^2\delta^2 + \zeta^4\right) \\ & - k_3\chi(\sigma^2 - \delta^2)\zeta \\ & + k_4\chi^4 + \frac{1}{4}\chi^4 \ln \frac{\chi^4}{\chi_0^4} - \epsilon\chi^4 \ln\left(\frac{\sigma^2 - \delta^2}{\sigma_0^2\zeta_0}\zeta\right) \end{aligned} \quad (4)$$

where  $k_0 \dots k_4$  are numerical constants, and the vector meson self interaction is given by

$$\begin{aligned} \mathcal{L}_{Vec} = & -\frac{\chi^2}{2\chi_0^2}(m_\omega^2\omega^2 + m_\rho^2\rho^2) \\ & - g_4^4(\omega^4 + 6\beta\omega^2\rho^2 + \rho^4) + \dots \end{aligned} \quad (5)$$

Here we ignore the  $\phi$  meson as we only want to study the effect on nucleons (plus a single hyperon). The explicit chiral symmetry breaking term is given by

$$L_{SB} = m_\pi^2 f_\pi \sigma + \left(\sqrt{2}m_k^2 f_k - \frac{1}{\sqrt{2}}m_\pi^2 f_\pi\right) \zeta. \quad (6)$$

In the case of the baryonic octet we use an f-type coupling between the baryons and vector mesons, which yields coupling strengths as given by quark counting rules, i.e.  $g_{i\omega} = (n_q^i - n_{\bar{q}}^i)g_8^V$ ,  $g_{i\phi} = -(n_s^i - n_{\bar{s}}^i)\sqrt{2}g_8^V$ , where  $g_8^V$  denotes the vector coupling of the baryon octet and  $n^i$  the number of constituent quarks of species  $i$  in a given hadron. Here, we allow for some slight tuning of the isovector channel ( $g_{N\rho}$ ) to optimize the reproduction of isotopic chains.

Before performing a full-scale study of all known nuclei, several test nuclei are selected, six crucial parameters  $g_{N\omega}$ ,  $g_{N\rho}$ ,  $g_4^4$ ,  $\epsilon$ ,  $\beta$  and  $r$  are varied and the resulting nuclear binding energies are studied. These parameters are the nucleon- $\omega$  coupling  $g_{N\omega}$ , the nucleon- $\rho$  coupling  $g_{N\rho}$ ,  $g_4^4$ , which governs the self-interaction of the vector mesons and  $\epsilon$ , which governs a logarithmic term in the scalar meson self-interaction and is usually very small. The other two parameters are  $\beta$ , which controls mixing terms between the  $\omega$  and  $\rho$  meson, and the ratio  $r$ , which controls how much of the mass of the vector meson is generated by the scalar fields ( $r=1$ ). In this way a parametrization is identified that best describes nuclear binding energies.

The test nuclei used for this approach are a general set from light to heavy nuclei, containing  $^{16}\text{O}$ ,  $^{40}\text{Ca}$ ,  $^{48}\text{Ca}$ ,  $^{58}\text{Ni}$ ,  $^{90}\text{Zr}$ ,  $^{116}\text{Sn}$ ,  $^{124}\text{Sn}$  and  $^{208}\text{Pb}$ , a set for moderately heavy nuclei, containing  $^{100}\text{Sn}$ ,  $^{110}\text{Sn}$ ,  $^{116}\text{Sn}$ ,  $^{120}\text{Sn}$ ,  $^{124}\text{Sn}$ ,  $^{130}\text{Sn}$ ,  $^{132}\text{Sn}$  and  $^{134}\text{Sn}$ , and a set for heavy nuclei, containing  $^{182}\text{Pb}$ ,  $^{186}\text{Pb}$ ,  $^{192}\text{Pb}$ ,  $^{202}\text{Pb}$ ,  $^{208}\text{Pb}$ ,  $^{212}\text{Pb}$  and  $^{214}\text{Pb}$ .

After a good parametrization was found, the whole even-even nuclei from the Wang-Audi-Wapstra data [20], [21], [22], [23], [24] were calculated, leading to an average error in the description of binding energies of 0.44%. The resulting values for the parameters are listed in table I

| Parameter     | Value  |
|---------------|--------|
| $g_{N\Omega}$ | 11.75  |
| $g_{N\rho}$   | 4.385  |
| $g_4^4$       | 38.75  |
| $\epsilon$    | 0.0607 |
| $\beta$       | 0      |
| $r$           | 0.5    |

TABLE I: Parameters of the TS2 model parametrization.

and shall hence be called TS2. Additionally, the model properties were tested in other realms such as the equation of state with a compressibility  $\kappa = 275.13$  MeV and hyperon potentials at saturation density ( $\Lambda = -29.2$  MeV,  $\Sigma^+ = 5.6$  MeV,  $\Xi^0 = -19.5$  MeV).

A main motivation for refitting the model parameters was the attempt to reproduce the masses of observed high-mass neutron stars. These observations give valuable insight how the equation of state behaves at very large densities. To check the star masses, the Tolmann-Oppenheimer-Volkoff equations for spherical stars was solved with this parametrization. The maximum mass of a neutron star within this model is  $2.05 M_\odot$  at a radius of 12 km (see figure 1). The maximum central density reached in the core is  $\sim 5.5 \rho_0$ . As such, the model is in accordance with current constraints on the neutron star mass-radius relation.

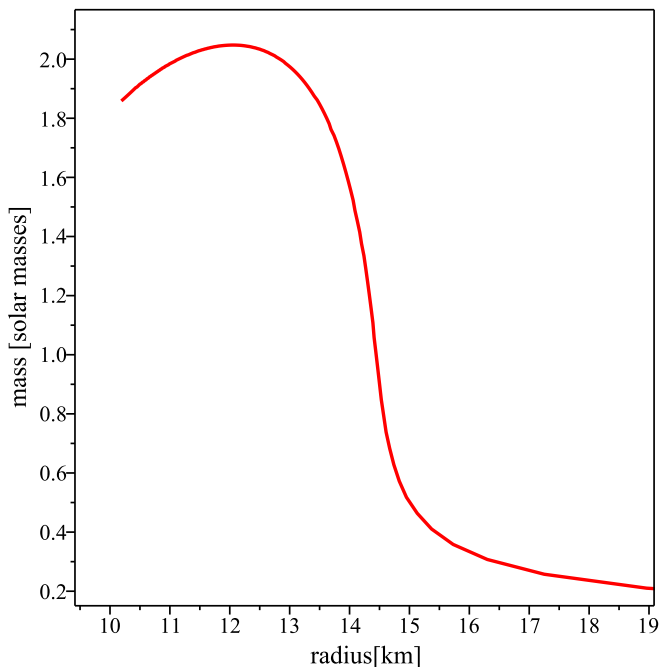


FIG. 1: Resulting mass-radius relation for neutron stars when applying the equation of state.

### III. RESULTS

We will now discuss the results obtained for the dripline calculations of the magnesium and magnesium +  $\Lambda$  hypernucleus isotope chain. As a first test, known one- $\Lambda$  separation energies of already measured hypernuclei were checked. We find that all three models give reasonable values about 0.5 to 1 MeV around the experimental values.

| Nucleus                | Experiment | NL3    | SPL40  | TS2    |
|------------------------|------------|--------|--------|--------|
| ${}^4_{\Lambda}H$      | 2.04       | 2.116  | 2.729  | 2.179  |
| ${}^9_{\Lambda}Li$     | 8.50       | 9.077  | 9.683  | 8.209  |
| ${}^{17}_{\Lambda}O$   | 13.59      | 12.688 | 12.854 | 12.260 |
| ${}^{41}_{\Lambda}Ca$  | 19.24      | 19.053 | 18.542 | 17.901 |
| ${}^{56}_{\Lambda}Fe$  | 21.00      | 22.356 | 22.356 | 20.362 |
| ${}^{139}_{\Lambda}La$ | 23.8       | 24.950 | 24.202 | 24.184 |
| ${}^{208}_{\Lambda}Pb$ | 26.5       | 26.310 | 25.183 | 25.432 |

TABLE II:  $\Lambda$  separation energies in MeV for various nuclei and models tested. For the experimental values, see [33] and references therein. The calculated results are from the NL3, SPL40 and TS2 models.

Please note that there exist both conventions in the literature,  $A=N+Z$  and  $A=N+Z+Y$ , with  $A$  denoting the nucleon or baryon number, respectively. We use the former one,  $A=N+Z$ , where the  $\Lambda$  is mentioned, but not counted.

For the dripline calculations, we use a two-dimensional code [17] to solve for the binding energy as a function

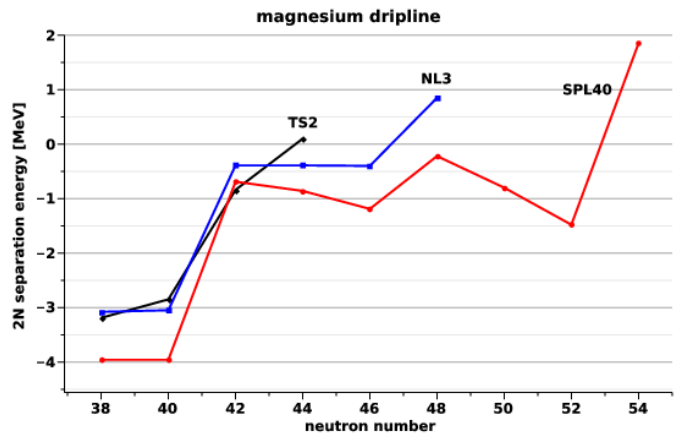


FIG. 2: 2-neutron separation energy  $S_{2n}$  for the magnesium chain within the various models. As long as the energy is negative, it means that the next nucleus is more deeply bound. A sign chain indicates instability with respect to neutron emission.

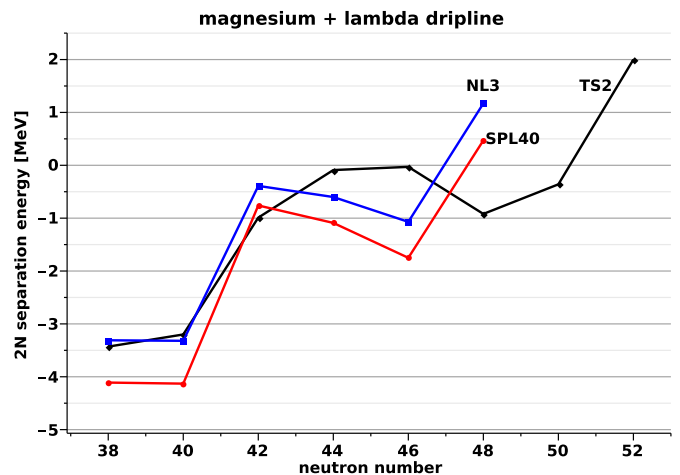


FIG. 3: 2-neutron separation energy  $S_{2n}$  for the magnesium chain plus a  $\Lambda$  hyperon added for the various models.

of the deformation of the nucleus. It is possible that several minima arise at prolate or oblate deformation, and the deepest minimum represents the energetically most stable configuration of the nucleus within the model approximations.

As long as the drip line is not reached, the addition of a neutron increases the binding energy of a nucleus but makes it more and more unstable. When the dripline is reached, the system cannot gain any energetic advantage anymore from adding another neutron. Hence the binding energy of the first unbound nucleus will be above the minimum of the binding energy of the last bound nucleus. In this way, the dripline can be calculated, which is analogous to looking for a sign change of the neutron separation energy  $S_{2n}$  ( $2n$  in this case as we only consider even-even nuclei).

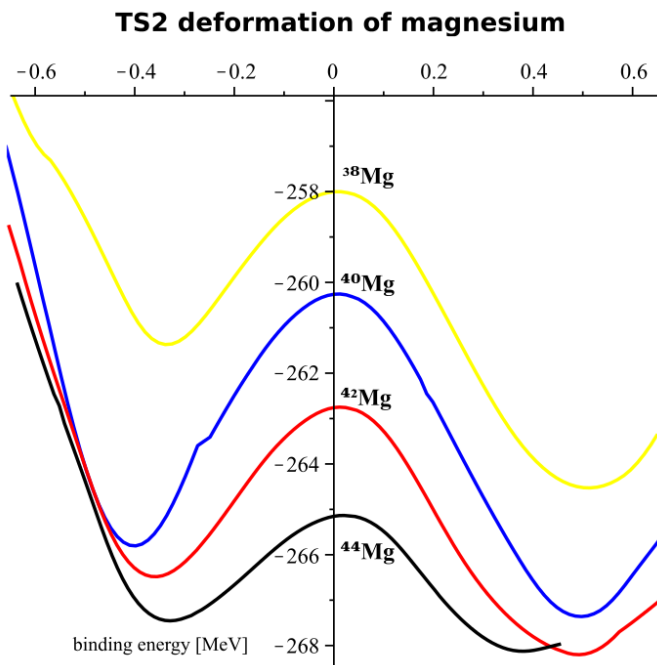


FIG. 4: Dripline calculation for Mg in the TS2 parameter set. The dripline is at  $^{42}\text{Mg}$ , as by a slight margin it is deeper bound than  $^{44}\text{Mg}$ . Plotted is the deformation on the x axis and the total binding energy in [MeV] on the y axis.

Figures 2 and 3 show the sign change and hence, the appearance of the dripline, for the magnesium and magnesium +  $\Lambda$  isotope chain. Within our model, we can also calculate the binding energy as a function of a specific deformation. This gives additional insight into the microscopic structure of the nucleus, and differs from simple liquid drop type calculations.

Overall, the general structure of the binding energy as function of deformation with resulting competing oblate and prolate minima is in accordance with other calculations [17, 25, 26].

Figures 4 and 5 show the important portion of the calculation where the dripline is reached for both the Mg and Mg +  $\Lambda$  isotope chain. It is noteworthy that the last experimentally measured nucleus of the Mg isotope chain is  $^{40}\text{Mg}$  [27]. In the TS2 model, we find that the dripline is at  $^{42}\text{Mg}$ . If a  $\Lambda$  hyperon is added, this opens up an additional degree of freedom, allowing for a wider energy distribution and the addition of eight additional neutrons, leading to a dripline at  $^{50}_{\Lambda}\text{Mg}$ . The general behavior of additional binding is expected in hypernuclei, however the size of the shift is quite remarkable.

When redoing the calculations for the SPL-40 and NL3 parameter sets, the driplines are found to be  $^{52}\text{Mg}$  and  $^{46}_{\Lambda}\text{Mg}$  for SPL-40 and  $^{46}\text{Mg}$  and  $^{46}_{\Lambda}\text{Mg}$  for the NL3 parameter set.

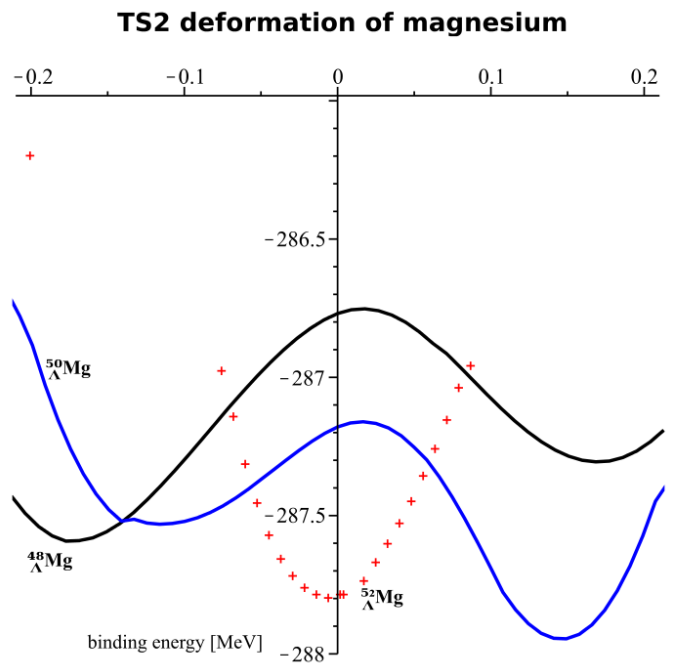


FIG. 5: Dripline for Mg with  $\Lambda$  in the TS2 parameter set. The dripline is at  $^{50}_{\Lambda}\text{Mg}$ . Plotted is the deformation on the x axis and the total binding energy in [MeV] on the y axis.

#### IV. DISCUSSION AND CONCLUSION

The calculations of the stability region of Mg and Mg+ $\Lambda$  show significantly different results for various models. All models predict the  $\Lambda$  separation energies of known hypernuclei with good precision, see table II.

When it comes to extrapolating to not yet experimentally measured hypernuclei, results become very model dependent. The SPL-40 parameter shows a rather interesting behavior. In contrast to the common conception that the addition of a hyperon does open up a new energy pool and hence, allows more neutrons to be present up to the fermi surface, here the opposite is the case. Instead, the system becomes unstable and, if created, would eject six neutrons to again reach the drip line.

Such a behavior would be very interesting. However, we do not observe similar results with other models. Both the NL3 and TS2 model confirm the general assumption that the addition of a  $\Lambda$  makes the nucleus more stable. However, all three models give different results for the position of the dripline. In the NL3 model, the addition of a  $\Lambda$  hyperon only changes the overall binding energy, but not the position of the dripline. In the TS2 model, the dripline changes from  $^{42}\text{Mg}$  to  $^{50}_{\Lambda}\text{Mg}$  when a  $\Lambda$  is added. When looking at the 2N separation energies, figure 3, the energy becomes almost zero for the TS2 model around  $^{44}_{\Lambda}\text{Mg}$  and  $^{46}_{\Lambda}\text{Mg}$ , but has a notable difference for  $^{48}_{\Lambda}\text{Mg}$  again. This could hint that, depending on the resolution ability of the model, the dripline could also occur

earlier, at  ${}^{44}_{\Lambda}Mg$  or  ${}^{46}_{\Lambda}Mg$ .

Summarizing, in this paper we have presented a new parameterisation of a chiral flavor-SU(3) Lagrangian that yields a good fit to nuclei as well as reproducing 2-solar-mass neutron stars. Specifically, we presented the isotope chain of Mg nuclei and the corresponding hypernuclei and compared results with other relativistic mean-field approaches. While all three models describe known low-mass hyper-nuclear  $\Lambda$  separation energies with good precision, the extrapolation to more neutron-rich nuclei

remains theoretically challenging. Therefore, a main result of the study is that such extrapolations to the dripline have found to be very model-dependent. As an intriguing result we have further shown that the stability of neutron-rich nuclei can be substantially modified by adding a  $\Lambda$ -hyperon, possibly shifting the drip-lines considerably by up to 8 neutrons.

Chhanda Samanta kindly acknowledges support provided by the LOEWE-Program (HIC-FAIR).

- 
- [1] H. Sugimura et al., *Search for  ${}^6_{\Lambda}H$  hypernucleus by the  ${}^6Li(\pi^-, K^+)$  reaction at  $p_{\pi^-} = 1.2$  GeV/c*, Phys. Lett. B **729**, 39 (2014); arXiv:1310.6104
- [2] Sugimura et al., *Study of Neutron-Rich Hypernuclei by the  $(\pi^-, K^+)$  Reaction at J-PARC*, Few Body Syst., **54**, 1235 (2013).
- [3] T. Gogami et al., *Electroproduction of  $K+\Lambda$  at JLab Hall-C*, Few Body Syst. **54**, 1227 (2013)
- [4] S.N. Nakamura et al., *Spectroscopic investigation of  $\Lambda$  hypernuclei in the wide mass region using the  $(e, e'K^+)$  reaction*, Jour. of Phys. **312**, 092047 (2011)
- [5] S. Bianchin et al., *The HypHI project: Hypernuclear spectroscopy with stable heavy ion beams and rare isotope beams at GSI and FAIR*, Int. J. Mod. Phys. E **18**, 2187 (2009); arXiv:0812.4148v1
- [6] T.R. Saito et al., *Latest Results From the HypHI Experiments at GSI: Hypernuclear Spectroscopy with Heavy Ion Induced Reactions*, Few-Body Syst. **54**, 1211 (2013).
- [7] A. S. Botvina, *Production of exotic hypernuclei and hyper-matter*, arXiv:1305.5474v1
- [8] Josef Pochodzalla, *Hypernuclei - the next decade*, Acta Phys.Pol B **42**, 833 (2011); arXiv:1101.2790v1
- [9] P.G.Reinhard, Z. Phys. A. **329**, 257 (1988).
- [10] K. Rutz, M. Bender, T. Bürvenich, T. Schilling, P.-G. Reinhard, J. A. Maruhn, W. Greiner, *Superheavy nuclei in self-consistent nuclear calculations*, Phys. Rev. C **56**, 238 (1997).
- [11] G. A. Lalazissis, A.R. Farhan, M. M. Sharma, Nucl. Phys. A. **628**, 221 (1998).
- [12] Panajotis Papazoglou, Stefan Schramm, Jürgen Schaffner-Bielich, Horst Stöcker, Walter Greiner, *Chiral Lagrangian for strange hadronic matter*, Phys. Rev. **57**, 2576 (1998).
- [13] P. Papazoglou, D. Zschesche, S. Schramm, J. Schaffner-Bielich, H. Stöcker, W. Greiner, *Nuclei in a Chiral SU(3) model*, Phys. Rev. C **59**, 411 (1999); arXiv: nucl-th/9806087
- [14] D. Zschesche, P. Papazoglou, S. Schramm, J.Schaffner-Bielich, H. Stöcker, W. Greiner, *Hadrons in Dense Resonance-Matter: A Chiral SU(3) Approach*, Phys. Rev. C **63**, 025211 (2001); arXiv: nucl-th:0001055
- [15] D. Zschesche, G. Zeeb, S. Schramm, H. Stöcker, *Impact of baryon resonances on the chiral phase transition at finite temperatures and density*, J.Phys.G **31**, 935 (2005); arXiv:nucl-th/0407117v2
- [16] V. A. Dexheimer, S. Schramm, *A novel approach to model hybrid stars*, Phys.Rev.C **81** 045201,(2010); arXiv:0901.1748v4
- [17] S. Schramm, *Deformed nuclei in a chiral model*, Phys.Rev. C **66**, 064310 (2002); arXiv:nucl-th/0207060v1
- [18] P. B. Demorest, T. Pennucci, S. M. Ramson, M. S. E. Roberts, J. W. T. Hessels, *A two-solar mass neutron star measured using Shapiro delay*, Nature, **467**, 1081 (2010).
- [19] John Antoniadis et al., *A massive pulsar in a compact relativistic binary*, Science **340** (2013)
- [20] G. Audi and A.H. Wapstra (1995), *The 1995 Update to the Atomic Mass Evaluation*, Nuclear Physics A **595**, 409 (1995).
- [21] G. Audi, O. Bersillon, J. Blachot and A. H. Wapstra, Nucl. Phys. A **729**, 3 (2003); G.Audi, A.H.Wapstra and C.Thibault, Nucl. Phys. A **729**, 129 (2003); G.Audi, A.H.Wapstra and C.Thibault, Nucl. Phys. A **729**, 337 (2003).
- [22] Audi, G., Kondev, F., Wang, M., Pfeiffer, B., Sun, X., Blachot, J., MacCormick, M., *The NUBASE2012 evaluation of nuclear properties*, Chinese Physics C **36**, 1157 (2012).
- [23] Audi, G., Wang, M., Wapstra, A., Kondev, F., MacCormick, M., Xu, X., Pfeiffer, B., *The AME2012 atomic mass evaluation (I). Evaluation of input data, adjustment procedures*, Chinese Physics C **36**, 1287 (2012).
- [24] Wang, M., Audi, G., Wapstra, A., Kondev, F., MacCormick, M., Xu, X., Pfeiffer, B., *The AME2012 atomic mass evaluation (II). Tables, graphs and references*, Chinese Physics C, **36**, 1603 (2012).
- [25] G. A. Lalazissis and P. Ring, *Excitation energy of superdeformed bands in relativistic mean field theory*, Phys.Lett. B **427**, 225 (1998).
- [26] R. Rodriguez-Guzman, J. L. Egido and L. M. Robledo, *Correlations beyond the mean field in magnesium isotopes: Angular momentum projection and configuration mixing*, Nucl. Phys. A **709**, 201 (2002).
- [27] T. Baumann, A. M. Amthor, D. Bazin, B. A. Brown, C. M. Folden III, A. Gade, T. N. Ginter, M. Hausmann, M. Matos, D. J. Morrissey, M. Portillo, A. Schiller, B. M. Sherrill, A. Stolz, O. B. Tarasov, M. Thoennessen, *Discovery of  ${}^{40}Mg$  and  ${}^{42}Al$  suggests neutron drip-line slant towards heavier isotopes*, Nature, **449**, 1022 (2007).
- [28] S. Schramm, *Nuclear and neutron star radii*, Phys.Lett. B **560**, 164 (2003); arXiv:nucl-th/0210053
- [29] Veronica Dexheimer, Stefan Schramm, *Proto-neutron and neutron stars in a chiral SU(3) model*, Astrophys.J. **683**, 943 (2008); arXiv:0802.1999
- [30] S.Schramm, D. Zschesche, *Rotating neutron stars in a chiral SU(3) model*, J.Phys.G **29**, 531 (2003); arXiv:nucl-th/0204075
- [31] Ch. Beckmann, P. Papazoglou, D. Zschesche, S. Schramm, H. Stöcker, W. Greiner, *Nuclei, super-*



- heavy nuclei and hypermatter in a chiral  $SU(3)$ -model*, Phys.Rev. C **65**, 024301 (2002) 024301; arXiv:nucl-th/0106014v1
- [32] Torsten Schürhoff, Stefan Schramm, *Neutron stars with small radii – the role of delta resonances* Astrophysical Journal Letters **724**, L74 (2010). [arXiv:1008.0957v1]
- [33] C. Samanta, P. Roy Chowdhury, D.N. Basu, *Generalized mass formula for non-strange and hyper nuclei with  $SU(6)$  symmetry breaking*, J.Phys.G **32**, 363 (2006); arXiv:nucl-th/0504085v2
- [34] C. Samanta, *Generalized mass formula for non-strange, strange and multiply-strange nuclear systems*, J. Phys. G: Nucl. Part. Phys. **37**, 075104 (2010); arXiv:1003.4227v1
- [35] A. Banu, L. Trache et al., *Structure of  $^{23}\text{Al}$  from the one-proton breakup reaction and astrophysical implications*, Phys.Rev.C **84**, 015803 (2011); arXiv:1104.0675v2
- [36] H. Sugimura, M.Agnello, C. Samanta et al. (J-PARC E10 Collaboration), *Search for  ${}^6_\Lambda\text{H}$  hypernucleus by the  ${}^6\text{Li}(\Pi^-, K^+)$  reaction at  $p_{\pi^-} = 1.2\text{GeV}/c$* , Phys. Let. B **729**, 39 (2014).
- [37] M. Ukai, S. Ajimura et al.,  *$\gamma$ -ray spectroscopy of  ${}^6_\Lambda\text{O}$  and  ${}^{15}_\Lambda\text{N}$  hypernuclei via the  ${}^{16}\text{O}(K^-, \pi\gamma)$  reaction*, Phys. Rev. C **77**, 054315 (2008).
- [38] R. H. Dalitz, D. H. Davis, T. Motoba, D. N. Tovee, *Proton emitting  $\lambda$  states of  ${}^{16}_\Lambda\text{O}^*$* , Nuclear Physics A **625**, 71 (1997).
- [39] J. N. Hu, A. Li, H. Shen, H. Toki, *Quark mean field model for single and double  $\Lambda$  and  $\Xi$  hypernuclei*, arXiv:1310.3602v1
- [40] J. Steinheimer, K. Gudima, A. Botvina, I. Mishustin, M. Bleicher, H. Stöcker, *Hypernuclei, dibaryon and antinuclei production in high energy heavy ion collisions: Thermal production vs. Coalescence*, Physics Letters B **714**, 85, (2012); arXiv:1203.2547v2
- [41] C. Albertus, J. E. Amaro, J. Nieves,  *$\Lambda\Lambda$  interaction and hypernuclei*, arXiv:1309.1484v1
- [42] Y. Tanimura, K. Hagino, *Description of single- $\Lambda$  hypernuclei with relativistic point coupling model*, arXiv:1111.1488v1